

## 【国外研修報告】

## AC Susceptibility Studies of Inter-grains in Hg-1223 Superconductors

N. Sakamoto\*, T. Akune\* and U. Ruppert\*\*

## Hg-1223 超伝導体におけるグレイン相間の交流帯磁率研究

坂本 進洋・阿久根 忠博・Udo Ruppert

**Abstract :** High- $T_c$  ceramics tend to lower its quality by the aging effect. The main cause of the degradation is considered to originate in the weak link region between the superconducting grains. The preservation and recovery of superconductivity by reinforcement of the grain boundary is an important issue for high-Tc application.

A quantitative analysis of the contribution due to the grain and the link is necessary and the grained Bean model is proposed, where the superconducting phases are immersed in the matrix link superconductor. Difference of the superconducting characteristics of the grain, the link and grain content factor give a variety of deformation on the AC susceptibility curves. Comparing the observed data with the numerically computed model allows more clear insight on the grain and inter-grain structures.

## 1. Introduction

Sintered high- $T_c$  superconductors exhibit two types of properties. One is intrinsic to the superconducting grains and the other is characteristic of the coupling between either grains. In such materials, the coupling component supports supercurrents and has its own effective critical temperature  $T_{ct}$ , critical current density  $J_{cl}$  and pinning penetration depth  $B_{pt}$ . The situation is less certain, but lack of stoichiometry at the grain boundaries and microbridges between grains give rise to a proximity-effect coupling. The coupling region shows a weak superconductivity and the field penetrates more freely through them compared to the grain region. Then the surface field of the grain is determined by the coupling matrix superconducting region. The intrinsic superconductors with high pinning penetration

field  $B_{pg}$  are considered to be immersed in the weak matrix with low  $B_{pt}$ .

Field distribution and magnetization in multiphases are calculated by Bean model [1]. Fourier integration of magnetization is carried out numerically and gives rise to the real part  $\chi'$  and the imaginary part  $\chi''$  of AC susceptibilities. Measured results of Re-doped Hg-1223 superconductors [2] are compared with the simulated results to give the link characteristics.

## 2. Grained Bean Model

Matrix superconductor with a penetration field  $B_{p0}$  determines the magnetic fields at the grain surface with the penetration field  $B_{pg}$  as shown in figure 1. Field distribution  $B_{oi}$  outside the  $i$ -th grain at a grain position  $X_i$  and field inside  $B_i$  of  $i$ -th grain with the grain size  $d_{gi}$  are

\* Department of Electrical Engineering and Information Technology, Kyushu Sangyo University, 2-3-1 Matsukadai, Fukuoka 813-8503, Japan

\*\* Tieftemperaturlabor, Fachbereich Physik, Freie Universitat Berlin, 14 Arnimallee, Berlin D-14195, Germany

given by using  $B_{p\ell}$ ,  $B_{pg}$  and Bean model as [3, 4]

$$B_{oi} = B_o - B_{p\ell} \left( \frac{X_i}{D} \right); \text{ outside the grain,} \quad (1)$$

$$B_i = B_{oi} - B_{pg} \left( \frac{x}{d_{gi}} \right); \text{ inside the grain,} \quad (2)$$

where  $D$  is a half thickness of the superconductor,  $x$  is a position inside the grain from the each grain surface as shown in the inset. Average of the magnetic flux density  $\langle B \rangle$  in the increasing period for both of the matrix and  $n_g$  grains with grain interval  $d_{vi}$  is given by

$$\langle B \rangle = B_o - \frac{B_p}{2} + \sum_{i=1}^{n_g} \left( \frac{d_{gi}}{d_{vi}} \right) m_i \quad (3)$$

Grain magnetization  $m_i$  is easily computed following magnetization process of each grains. In the case of uniform grain structure with constant grain size  $d_g (= d_{gi} \text{ for all } i)$  and inter-grain distance  $d_v (= d_{vi} \text{ for all } i)$ , where  $f_g (= d_g / d_v)$  is the grain content factor. Then the magnetization  $M$  of the superconductor at the field  $B_o$  for each magnetization processes is given by

$$M = \langle B \rangle - B_o = -\frac{B_p}{2} + f_g \sum_{i=1}^{n_g} m_i \quad (4)$$

The equations for the AC susceptibilities  $\chi'$  and  $\chi''$  under an AC field  $B_a \cos \omega t$  are derived from Fourier integrals of the magnetization. The fundamental Fourier components  $\chi_1'$  and  $\chi_1''$  are denoted as  $\chi'$  and  $\chi''$  hereafter, and expressed as [5]

$$\chi = \chi' + i\chi'' = \frac{1}{\pi B_a} \int_{-\pi}^{\pi} M \exp(i\omega t) d\omega t. \quad (5)$$

### 3. Results and discussion

Numerical integration of equation (5) is carried out and temperature dependence of  $\chi'$  and  $\chi''$  is obtained by introducing the temperature variation of the penetration fields of

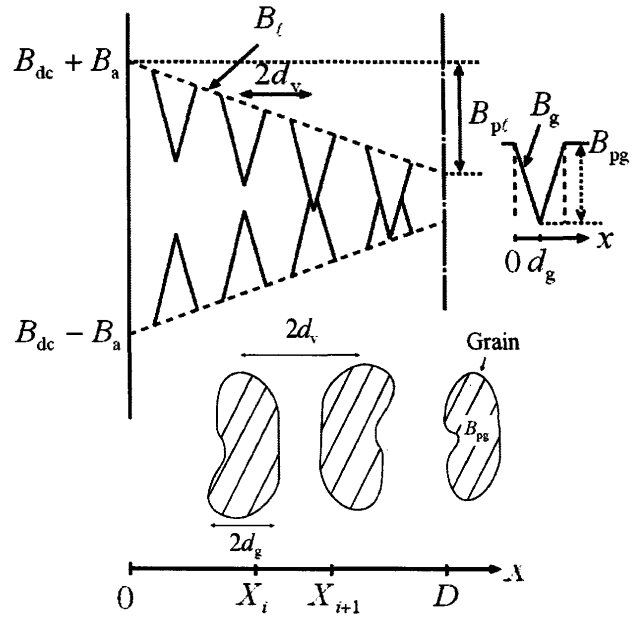


**Figure 1.** Field distribution  $B_{oi}$  outside the grain and distribution  $B_i$  inside the grain. Penetration fields are  $B_{p\ell}$  and  $B_{pg}$  for matrix and grain, respectively.

$B_{p\ell}$  and  $B_{pg}$ . If these  $B_{p\ell}, B_{pg}$ 's have a usual parabolic dependence of the form as,  $B_{p\ell, pg} = B_{p\ell, pg}(0) \left\{ 1 - (T/T_{cl, cg})^2 \right\}^{n_{\ell, n_g}}$ , where over the temperatures  $T_{cl}$  and  $T_{cg}$  the pinning effect for the fluxoid motion disappears in the link and the grain region, respectively.

The effect of  $B_{pg}$  are shown in figure 2 at a fixed grain content of  $f_g = 0.5$ , AC field amplitude  $B_a / B_{p\ell}(0) = 0.2$ ,  $n_g = 2$  and  $n_{\ell} = 6$ . The imaginary peaks decrease with increasing  $B_{pg}(0)$  and new peaks appear at higher temperature and coexist. This type of double peaks is often observed in high- $T_c$  materials [6]. The effect of  $B_{p\ell}$  are indicated in figure 3. The enhancement of  $B_{p\ell}(0)$  moves the lower peak to higher temperatures and unites to single peak at  $B_{p\ell}(0) = B_{pg}(0)$ . The double peak structure in the  $\chi''$  curve is specifically indicated to originate in the cooperative work of the grain and the interconnecting link.

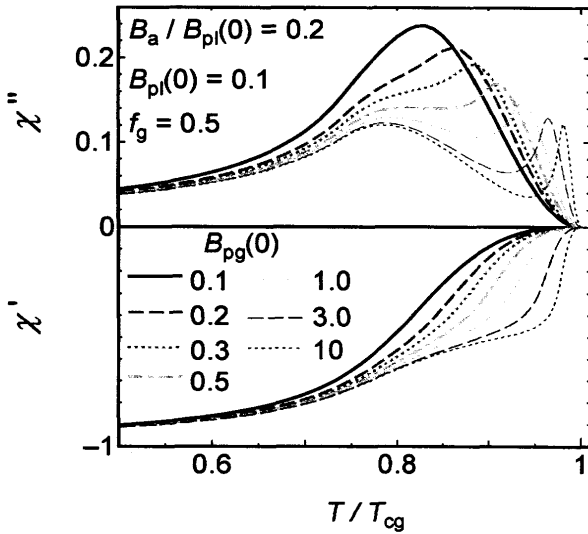


**Figure 2.** Dependence of AC susceptibilities  $\chi'$  and  $\chi''$  on reduced temperature  $T/T_{cg}$  with grain penetration field at 0 K,  $B_{pg}(0)$  of 0.1, 0.2, 0.3, 0.5, 1.0, 3.0 and 10 at a grain content of  $f_g = 0.5$ .

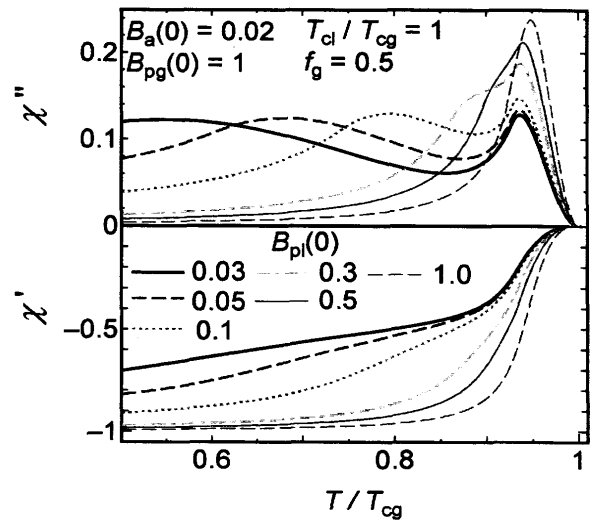


**Figure 3.** Dependence of AC susceptibilities  $\chi'$  and  $\chi''$  on reduced temperature  $T/T_{cg}$  with link penetration field at 0 K,  $B_{pl}(0)$  of 0.03, 0.05, 0.1, 0.3, 0.5 and 1.0.

#### 4. Grain and link characteristics in Hg-1223 superconductors

The double peak characteristics of HgBa<sub>2</sub>Ca<sub>2</sub>Cu<sub>3</sub>Re<sub>0.15</sub>O<sub>8+δ</sub> (Hg-Re-15c) powdered sample [2] are shown in figure 4 (a), where temperatures are normalized by the critical temperature  $T_c(B_{dc})$  at the applied DC magnetic field  $B_{dc}$ . The computed results by the grained Bean model are plotted in figure 4 (b) and explained well the experimental results. The fitting parameters are listed in table 1. The link region shows a large temperature change with indices  $n_b = 6$  compared with  $n_g = 2$ . A decrease of volume factor of the grain region  $f_g$  with

increasing  $B_{dc}$  may imply the weakness of the grain surfaces.

#### 5. Conclusions

Textures of grains and interconnecting links in high- $T_c$  superconductors are simulated by the grained Bean model, where the superconducting regions are divided two parts; grains and interconnecting links. A variety of characteristics, double peak in the imaginary part of AC susceptibility and their movement are shown in the computed results. Double peak characteristics were successfully analyzed by the grained Bean model.

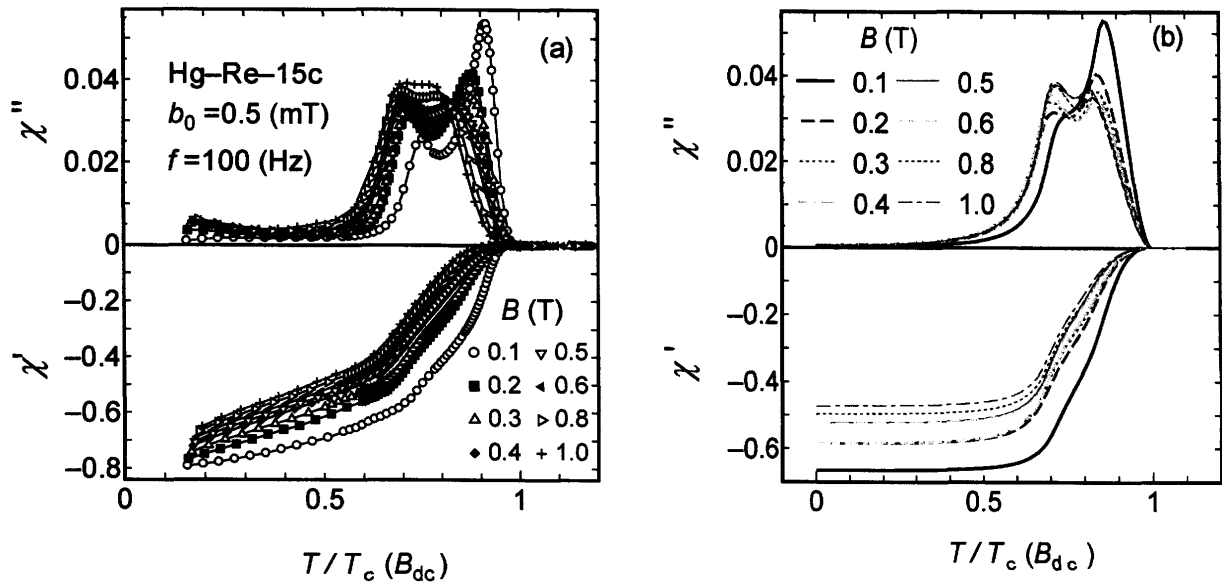


**Figure 4.** (a) Temperature dependence of AC susceptibilities of  $\text{HgBa}_2\text{Ca}_2\text{Cu}_3\text{Re}_{0.15}\text{O}_{8+\delta}$  powdered sample. (b) Numerically computed AC susceptibilities as a function of  $T/T_c(B_{dc})$  for fields of 0.1-1.0 T.

Table 1. Fitting parameters.

$B$ (T)	$B_{pg}(0)/B_a$	$B_{pl}(0)/B_a$	$f_g$	$B_{pg}$ (mT)	$B_{pl}$ (mT)
0.1	11.67	58.3	0.76	5.83	29.2
0.2	9.17	37.5	0.65	4.58	18.8
0.3	9.17	37.5	0.58	4.58	18.8
0.4	9.17	40.0	0.55	4.58	20.0
0.5	7.50	44.0	0.55	3.75	22.0
0.6	8.50	48.0	0.53	4.25	24.0
0.8	8.30	46.0	0.53	4.15	23.0
1.0	7.50	45.0	0.53	3.75	22.5

## References

- [1] Bean C P 1962 *Phys. Rev. Lett.* **8** 250
- [2] Yamada N, Akune T, Sakamoto N and Matsumoto Y 2004 *Physica C* **412-414** 425
- [3] Kubo M, Akune T and Sakamoto N, to be published in *Physica C*
- [4] Yumoto W, Akune T and Sakamoto N 2007 *Annual Report of RISS* [in Japanese] **4** 86
- [5] Matsushita T, Otabe E S and Ni B 1991 *Physica C* **182** 95
- [6] Fàbrega L, Sin A, Calleja A and Fontcuberta J 2000 *Phys. Rev. B* **61** 9793